BBA - Biomembranes 1860 (2018) 2428–2435

Contents lists available at ScienceDirect

BBA - Biomembranes

journal homepage: www.elsevier.com/locate/bbamem

Cerium oxide nanoparticles as potential antibiotic adjuvant. Effects of CeO_2 nanoparticles on bacterial outer membrane permeability

Pierangelo Bellio[a,*], Carla Luzi[a], Alisia Mancini[a], Salvatore Cracchiolo[a], Maurizio Passacantando[b], Letizia Di Pietro[a], Mariagrazia Perilli[a], Gianfranco Amicosante[a], Sandro Santucci[b], Giuseppe Celenza[a]

[a] Department of Biotechnological and Applied Clinical Sciences, University of l'Aquila, via Vetoio, 67100 L'Aquila, Italy
[b] Department of Physical and Chemical Sciences, University of L'Aquila, via Vetoio, 67100 L'Aquila, Italy

ARTICLE INFO

Keywords:
CeO_2 nanoparticles
Drug synergism
Antimicrobial resistance
Bliss independence theory
KPC beta-lactamase
K. pneumoniae

ABSTRACT

Background: Therapeutic options against Multi Drug Resistant (MDR) pathogens are limited and the overall strategy would be the development of adjuvants able to enhance the activity of therapeutically available antibiotics. Non-specific outer membrane permeabilizer, like metal-oxide nanoparticles, can be used to increase the activity of antibiotics in drug-resistant pathogens. The study aims to investigate the effect of cerium oxide nanoparticles (CeO_2 NPs) on bacterial outer membrane permeability and their application in increasing the antibacterial activity of antibiotics against MDR pathogens.

Methods: The ability of CeO_2 NPs to permeabilize Gram-negative bacterial outer membrane was investigated by calcein-loaded liposomes. The extent of the damage was evaluated using lipid vesicles loaded with FITC-dextran probes. The effect on bacterial outer membrane was evaluated by measuring the coefficient of permeability at increasing concentrations of CeO_2 NPs. The interaction between CeO_2 NPs and beta-lactams was evaluated by chequerboard assay against a *Klebsiella pneumoniae* clinical isolate expressing high levels of resistance against those antibiotics.

Results: Calcein leakage increases as NPs concentrations increase while no leakage was observed in FITC-dextran loaded liposomes. In *Escherichia coli* the outer membrane permeability coefficient increases in presence of CeO_2 NPs. The antibacterial activity of beta-lactam antibiotics against *K. pneumoniae* was enhanced when combined with NPs.

Conclusions: CeO_2 NPs increases the effectiveness of antimicrobials which activity is compromised by drug resistance mechanisms. The synergistic effect is the result of the interaction of NPs with the bacterial outer membrane. The low toxicity of CeO_2 NPs makes them attractive as antibiotic adjuvants against MDR pathogens.

1. Introduction

The phenomenon of antimicrobial resistance has emerged among pathogenic bacteria since the beginning of the antibiotic era as consequence of the selective pressure generated by the use, abuse and misuse of antibiotics in human and veterinary medicine. Nowadays, pathogenic organisms expressing Multi Drug Resistance (MDR) phenotype are among the most important cause of infections in nosocomial and community settings. Therapeutic options for infections sustained by MDR pathogens are limited and often ineffective, and new drugs are urgently needed [1]. To overcome antibiotic-mediated resistance, the overall strategy would be, so far, the use of combinations of drugs or the development of adjuvants that, acting in concert with licensed agents, can enhance their antimicrobial activity even against resistant strains. Substances able to increase susceptibility to currently licensed agents, would be very attractive and useful [2–4].

The development of antibiotic adjuvants does not necessarily imply the discovery of new targets in bacterial cells, on the contrary, most of the known cell targets can be exploited (*e.g.* beta-lactamase inhibitors), or even non-specific compounds like outer membrane permeabilizer can be used to increase the activity of antibiotics. Outer membrane in Gram-negative bacteria is a semipermeable barrier that confers inherent resistance to most antibiotics [5,6]. The entrance of hydrophilic antibiotics such as beta-lactams, is allowed trough channel-forming proteins called porins which represent < 1% of the surface area. Moreover, the rate of uptake into the cell is often reduced by the

* Corresponding author.
E-mail address: pierangelo.bellio@univaq.it (P. Bellio).

https://doi.org/10.1016/j.bbamem.2018.07.002
Received 19 March 2018; Received in revised form 29 June 2018; Accepted 9 July 2018
Available online 17 July 2018

presence of efflux pumps, making actually the accessible area, ungenerous. The passage of hydrophobic compounds is also prevented by the presence in the outer layer of the outer membrane, of the polyanionic lipopolysaccharide (LPS) which is stabilised by divalent cations. The displacement of the stabilising cations operated by polycations such as polymyxins, aminoglycosides or cationic peptides [6] makes outer membrane increasingly permeable to other compounds [7]. Following this logic, positively-charged metal oxide nanoparticles (MeO-NPs) have been demonstrated firmly bind bacterial cell membrane [8].

In the last years the interest in MeO-NPs is enormously increased as potential antibacterial agents against drug-resistant pathogens [8]. The nanometer size of metal oxide NPs as the physical and chemical properties, are strictly related to their antimicrobial activity [9,10]. Specifically, ceria nanoparticles (NPs) have been extensively studied for a variety of potential applications in several fields, including nanomedicine [11–18]. Their ability to act as antioxidant has been well established [16,19–21], but investigations about their antimicrobial potentiality are still undergoing. Recently has been demonstrated that coated ceria NPs are able to inhibit up to 50% the growth of *Pseudomonas aeruginosa* bacterial strain [22]. Thill et al. [23] have demonstrated the cytotoxicity of CeO_2 NPs against the enterobacterial *Escherichia coli* and Shah et al. [12] demonstrated that dextran coated cerium oxide nanoparticles are able to induce toxicity against *Escherichia coli* [12,23]. Pelletier et al. [24] showed as cerium oxide NPs exert a moderate bactericidal activity against *E. coli* and *Bacillus subtilis*. Moreover, several studies demonstrated that morphology, size and composition of CeO_2 NPs surface, characterize their antibacterial properties [25–27].

Has been postulated that CeO_2 NPs adsorb *via* electrostatic attraction to the bacterial surface but do not penetrate them [23,24,28]. The electrostatic interaction between NPs and the membrane seems to be so strong that they might stick at the surface for a very long time [23] and Ce^{4+} atoms close to the membrane surface are reduced to Ce^{3+}, resulting in oxidative stress on the major components of the membrane such as lipids and/or proteins [23]. The oxidation of the bacterial cell would create mesosoma like structures, therefore several elementary and essential functions as DNA replication, cell division are changed and consequently the surface area of bacterial cell membrane is increased [29] properly because the formation of membrane invaginations. However, despite the attempts to demonstrate and ameliorate the toxic activity of ceria NPs against pathogenic bacteria [12,22–24,30], they still cannot be defined as pure and efficient antibacterial agents.

2. Materials and methods

2.1. Antibiotics and reagents

All tested antibiotics, cefotaxime (CTX), imipenem (IMP), amoxicillin (AMX) and clavulanate (CLV) were from Sigma-Aldrich (Milan, Italy). All reagents used for the preparation of ceria nanoparticles were from Sigma-Aldrich (Milan, Italy). Nitrocefin was kindly provided by professor Shahriar Mobashery laboratories (Notre Dame University, US-IN). *Escherichia coli* total lipid extract for calcein-entrapping liposomes preparation were from Avanti Polar Lipids (Alabaster, US-AL) and calcein was from Sigma-Aldrich (Milan, Italy). Fluorescein isothiocyanate dextran D-4, D-20 D-70 were from Sigma-Aldrich (Milan, Italy).

2.2. Organisms

Escherichia coli HB101, host cells (genotype, F- *mcrB mrr hsdS20(rB-mB-) recA13 leuB6 ara-14 proA2 lacY1 galK2 xyl-5 mtl-1 rpsL20(SmR) glnV44* λ-) from Promega (Madison, US-WI) were used for permeability assays.

Klebsiella pneumoniae carbapenemase (KPC)-producing, named KP1/11, was used for drug interaction assays [31]. The *K. pneumoniae* KP1/11 strain shows the simultaneous presence of the resistance genetic determinants bla_{KPC-3} and bla_{VIM-2} encoding for a serine-beta-lactamase and a metallo-beta-lactamase, respectively. Moreover, the presence of *aac*A29b and *aac*(6′)-Ib genes, confers resistance to aminoglycosides.

2.3. CeO_2 nanoparticles synthesis

Cerium oxide nanopowders were synthesised using a modified precipitation method with cerium nitrate hexahydrate as precursor [32]. The process of chemical synthesis, the structural and electronic properties of the nanoparticles of cerium oxide used in this study, were previously reported [33]. Specifically, CeO_2 NPs used in this work, were calcined in an air furnace at temperature T = 500 °C for 8 h.

2.4. Calcein loaded liposomes

Calcein-entrapping liposomes of different lipid compositions were prepared as previously described [34] with some modifications. Briefly, 1 mL of a solution of calcein 60 mM in sodium phosphate buffer 50 mM, pH 7.4, containing EDTA 0.1 mM, was cosonicated with 1 mL of *E. coli* total lipid extract dissolved in chloroform. After that, lipid vesicles were prepared by reverse phase evaporation method [35]. Untrapped calcein was removed by gel filtration (Sephadex G-50, 1.5 × 15 cm column, equilibrated and eluted with 50 mM sodium phosphate buffer, pH 7.4, containing 0.1 mM EDTA). The lipid concentration in the separated vesicular fractions was determined by the method of Stewart [36].

Lipid vesicles preloaded with calcein were treated with cerium oxide NPs at concentrations ranging from 50 μg/mL to 600 μg/mL in sodium phosphate buffer 50 mM, pH 7.4 and EDTA 0.1 mM. The release of calcein from liposomes was monitored fluorimetrically on a Perkin-Elmer LS 50 B spectrofluorimeter; excitation and emission wavelengths were 490 nm and 517 nm, respectively. The maximum fluorescence intensity was determined by the addition of 20 μL of a water solution of Triton X-100 (10%, v/v) to the sample containing calcein loaded liposomes.

The percentage of calcein released was calculated according to the equation [37]:

$$Leakage\ (\%) = 100 \times (F - F_0)/(F_t - F_0)$$

where F and F_t are the intensity of fluorescence before and after the addition of the detergent and F_0 is the fluorescence of intact vesicles.

2.5. Dextran loaded liposomes

Dextran loaded vesicles containing the FITC-D of choice (FITC-D 4, 20 or 70) were prepared as reported elsewhere [38]. The release of dextran from loaded vesicles upon interaction with cerium oxide NPs, at the same concentrations used for calcein loaded liposomes, was examined fluorimetrically; excitation and emission wavelengths were 494 nm and 520 nm, respectively. In a typical experiment, an aliquot of a solution of cerium NPs in potassium phosphate buffer 50 mM, pH 7.4 and EDTA 0.1 mM, was incubated 10 min with a suspension of dextran-loaded vesicles, with a final lipid concentration of 50 μM. The mixture was gently stirred for 10 min in the dark and then centrifuged at 22500*g* for 30 min. The supernatant was recovered, and its fluorescence intensity recorded. The maximum fluorescence intensity was determined by the addition of 20 μL of 10% (v/v) Triton X-100 water solution to the vesicle suspension. The apparent percentage leakage value was calculated as previously done for calcein. All experiments were carried out at room temperature and in triplicate.

2.6. Outer membrane permeability assay

Outer membrane permeability was determined as previously described by Zimmermann and Rosselet [39]. *E. coli* HB101 was transformed with the expression vector pBR322 containing the gene bla_{TEM-}

$_1$, encoding for the beta-lactamase TEM-1. The recombinant organism was grown overnight at 37 °C in 10 mL of Tryptic Soy Broth (TSB) containing 100 μg/mL of ampicillin. The starter culture was added to 100 mL of TSB pre-warmed at 37 °C and grown for 4 h until the optical density at 600 nm reached the value of 0.5–0.6 corresponding to an approximate bacterial concentration of 10^8–10^9 CFU/mL. The culture was centrifuged at 4.000 rpm for 10 min at room temperature and the pellet subsequently resuspended in 30 mL of phosphate buffer 0.1 M, pH 7.0 containing 0.9% of NaCl and 5 mM of $MgCl_2$. This step was repeated twice and finally, the pellet was resuspended in 18 mL of the same buffer. The bacterial suspension was divided in three aliquots: one was used as control, while the others were treated with several concentrations of cerium oxide NPs ranging from 1.56 μg/mL to 100 μg/mL. After 20 min incubation at 25 °C, each reaction was divided into further three aliquots; one was kept apart and used to determine the rate of nitrocefin hydrolysis in intact cells (v_{int}). The second aliquot was sonicated with three 30 s bursts at 100% of amplitude (0.5 cycle) and held at 4 °C and used to determine the substrate hydrolysis in sonically treated cells (v_{son}). The last portion was cleared of cells by centrifugation (4.000 rpm for 10 min at room temperature) and used to determine the residual activity of the supernatant (v_{sup}) due to possible leakage of the beta-lactamase. The initial rates v_{int}, v_{son} and v_{sup} were spectrophotometrically determined at 50 μM of nitrocefin (S_0), at 480 nm.

The kinetic parameters K_m and V_{max} for TEM-1 enzyme in sonicated cells, were determined by non-linear fitting of the Michaelis-Menten equation using nitrocefin concentrations ranging from 10 μM to 200 μM.

At a given substrate concentration outside the cell (S_0), the steady-state concentration of nitrocefin inside the periplasmic space (S_p) can be calculated rearranging the Michaelis-Menten equation as follows:

$$S_p = K_m \times v'_{int}/(V_{max} - v'_{int})$$

v'_{int} is the initial rate of the intact cells where the rate of nitrocefin hydrolysis of the supernatant (v_{sup}) is subtracted. The membrane permeability coefficient can be calculated rearranging the Fick's law of diffusion [40]:

$$C = v'_{int}/(S_0 - S_p)$$

2.7. In vitro susceptibility tests and chequerboard microdilution assay

The antimicrobial susceptibility pattern of the *K. pneumoniae* KP1/11 used in this study was determined in accordance with the CLSI guidelines [41]. In detail, 50 μL of each bacterial suspension in 0.9% saline solution (NaCl) were added to the wells of a sterile 96-well microtiter plate, already containing 50 μL of two-fold serially diluted antibiotic or CeO_2 NPs in cation-adjusted Mueller-Hinton, to reach a final volume in each well of 100 μL. Positive control wells were prepared with culture medium and bacterial suspension. Negative control wells were prepared with culture medium and antibiotic or CeO_2 NPs. The microtiter plates were incubated for 18 h at 37 °C. The growth in each well was quantified spectrophotometrically at 595 nm by a microplate reader iMark, BioRad (Milan, Italy). The minimum inhibitory concentration (MIC) for drugs and CeO_2 nanoparticles was defined as the concentration of drug that reduced growth by 80%, compared to that of organisms grown in absence of drug. MIC value was determined as the median of at least three independent experiments.

The *in vitro* interactions between the antibiotics and CeO_2 NPs were investigated by a two-dimensional chequerboard microdilution assay, using a 96-well microtitration plates as previously described with some modifications [42,43]. Briefly, a stock solution of antibiotics and CeO_2 NPs was prepared in Mueller-Hinton medium and serially diluted twofold in the same medium. Drug dilutions were initially prepared to obtain four times the final concentration. In each well of the microplate 25 μL of microbial growth medium were added. An aliquot of 25 μL of a fourfold concentrated antibiotic was added to column 12. Then a twofold dilution was made from column 12 to column 2. A 25 μL aliquot of each drug concentration of the compound was added to rows A to G. Row H contained only the antibiotic while column 1 only the compound. Well H1 was the drug free well used as growth control. Finally, 50 μL of a 0.9% saline solution containing bacteria were added to each well of the microplate to obtain a final *inoculum* of 5×10^5 CFU/mL. The microtiter plates were incubated at 37 °C for 18 h. The growth in each well was quantified spectrophotometrically at 595 nm by a microplate reader. The percentage of growth in each well was calculated as the ratio between the OD_{595nm} measured in the wells were drugs are present and the OD_{595nm} of the drug free well, after subtraction of the blank obtained from the microorganism-free plates, processed as the inoculated plates. The MICs for each combination of drugs were defined as the concentration of drug that reduced growth by 80% compared to that of organisms grown in the absence of drug. All experiments were performed in triplicate.

2.8. Drug interaction model

To assess the nature of the *in vitro* interactions between CeO_2 nanoparticles and beta-lactam antibiotics against *K. pneumoniae* KP1/11, the data obtained from the chequerboard assay were analysed by the Bliss independence (BI) theory [44]. In the Bliss models, the combined effects of the drugs calculated from the effect of the individual drugs, are compared with those obtained experimentally. The BI theory is described by the equation $I_i = I_A + I_B - I_A \times I_B$ where I_i is the predicted percentage of inhibition of the theoretical non-interactive combination of drug A and B and I_A and I_B are the experimental percentages of inhibition of each drug acting alone. Since the percentage of inhibition is equal to $I = 1 - E$, the former equation can be expressed as: $E_i = E_A \times E_B$, where E_i is the calculated percentage of growth based on the theoretical non-interactive combination of drug A and B, and E_A and E_B are the experimental percentages of growth of each drug acting alone.

The experimental dose-response surface is subtracted from the calculated theoretical surface to reveal any significant deviation from the zero-plane. Thus, the interaction is described by the difference (ΔE) between the predicted and measured percentages of growth with drugs at various concentrations ($\Delta E = E_{predicted} - E_{measured}$). To determine the significance of differences between the experimental and calculated additive effects, the upper and lower 95% confidence limits of the experimental data were compared to the calculated additive effects. If the lower confidence limit of a point was greater than the calculated additivity, the observed synergy was significant. Similarly, if the upper confidence limit was lower than the calculated additivity, the observed antagonism was significant [45,46]. The ΔE values calculated on a point-by-point basis were subsequently plotted on the *z* axis. Points of the difference surface above zero (positive) indicate synergy, below zero (negative) antagonism. To summarise the interaction surface, the Bliss synergy and antagonism differences and all their combinations were added up to yield a summary measure, respectively of Bliss synergy (ΣSYN) and Bliss antagonism (ΣANT). Interactions < 100% were considered weak, interactions between 100% and 200% were considered moderate, while interaction > 200% were considered strong [47].

2.9. Data analysis and statistics

Data were analysed using the software OriginPro ver. 8.5 (OriginLab Corporation, Northampton, MA, USA). All statistical analyses were performed with SigmaPlot ver. 11.0 (Systat Software Inc., Chicago, IL, USA). Data are presented as mean ± standard deviation (SD), of three independent determinations. Comparison of more than two group means was carried out by ANOVA test followed by Holm-Sidak test. Level of $p < 0.001$ was regarded as statistically significant.

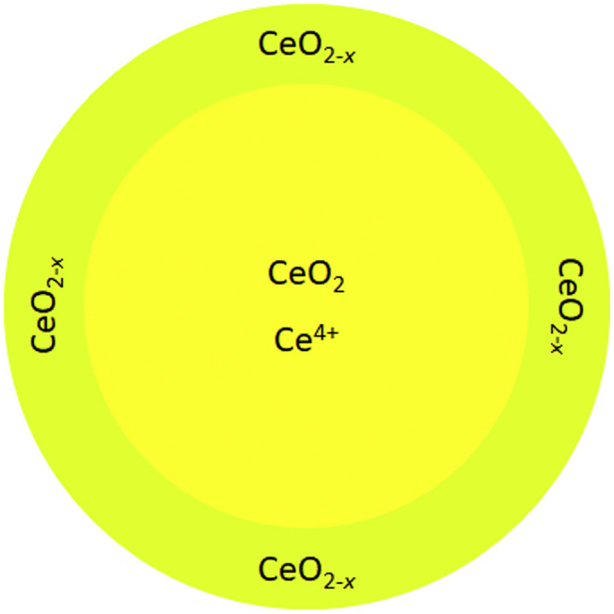

Fig. 1. Diagram of the CeO_{2-x} NPs composition.

3. Results

3.1. CeO_2 nanoparticles characterization

Cerium oxide nanoparticles were previously characterized by X-ray photoelectron spectroscopy (XPS) and X-ray diffraction (XRD) to determine their electronic and structural properties, respectively [33]. In particular, XPS data analysis showed a concentration of 24.7% relatively to the Ce^{3+} ions; XRD pattern showed that the NPs are single-phased and correspond to cubic phase fluorite-type CeO2 (JCPDS 034-0394) with a lattice parameter of 0.542 nm, larger than the bulk CeO_2 (0.541 nm), which dependents on the particle diameter size, that in this case is about 10 nm [33].

This discrepancy is due to more non-equilibrium conditions of preparation of CeO_{2-x} nanoparticles. In addition, has been demonstrated that the oxygen non-stoichiometry of nanoparticles increases from the middle to the surface (Fig. 1).

3.2. Calcein leakage assay in liposomes

To verify the ability of cerium oxide NPs to induce perturbation of membrane permeability, multilamellar liposomes were loaded with calcein, which fluorescence is quenched as the molecules are confined within the liposomal vesicles. Calcein is a relatively small molecule with a molecular weight of 622.55 Da; any perturbation of liposome membrane able to induce leakage of the vesicle content can be detected by following the increase in fluorescence intensity caused by calcein release. As shown in Fig. 2, the percentage of permeabilized liposomes increases in a dose-response manner when treated with increasing concentrations of cerium oxide NPs. The maximum percentage of leakage is reached at 400 μg/mL of cerium oxide NPs with almost the 80% of permeabilized liposomes.

3.3. Dextran loaded liposomes

With the aim to determine the entity of perturbation, dextran loaded liposomes were prepared. As in calcein leakage assay, the fluorescence of fluorescein isothiocyanate conjugate dextrans (FITC-dextrans) is quenched inside the vesicles, with the difference of the higher molecular weight of dextrans, with respect to calcein.

In this study, three different FITC-dextrans have been used: D-4, D-20 and D-70 with an average molecular weight of about 4, 20 and 70 kDa, respectively. The difference in molecular weights allows to determine the extent of the damages to the membrane by observing the size-dependent release of liposome-entrapped probes.

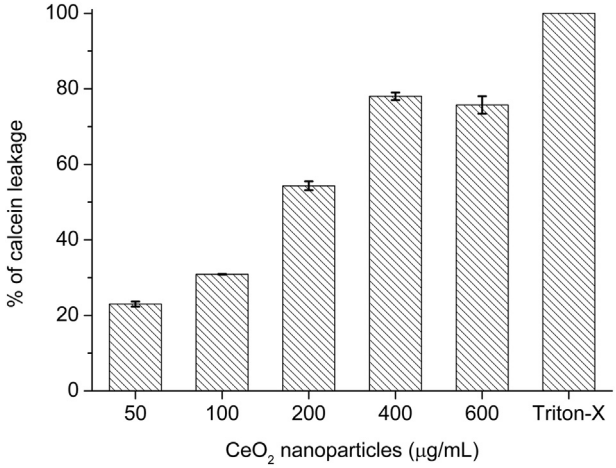

Fig. 2. Percentage of calcein leakage as function of CeO_2 nanoparticles concentration. Data are presented as mean ± standard deviation (SD).

As shown in Fig. 3, the percentage of permeabilized liposomes containing dextrans is low. For instance, the highest leakage can be observed in lipid vesicles containing D-4 probe, with a percentage of dextran leakage about 15% at the highest concentration of cerium oxide NPs (600 μg/mL) (Fig. 3A). In D-20 and D-70 loaded liposomes, even at the highest cerium oxide NPs concentration, no significant leakage can be observed (Fig. 3B and C): < 7% and about 2%, respectively.

3.4. Outer membrane permeability assay

The ability of cerium oxide NPs to alter outer membrane

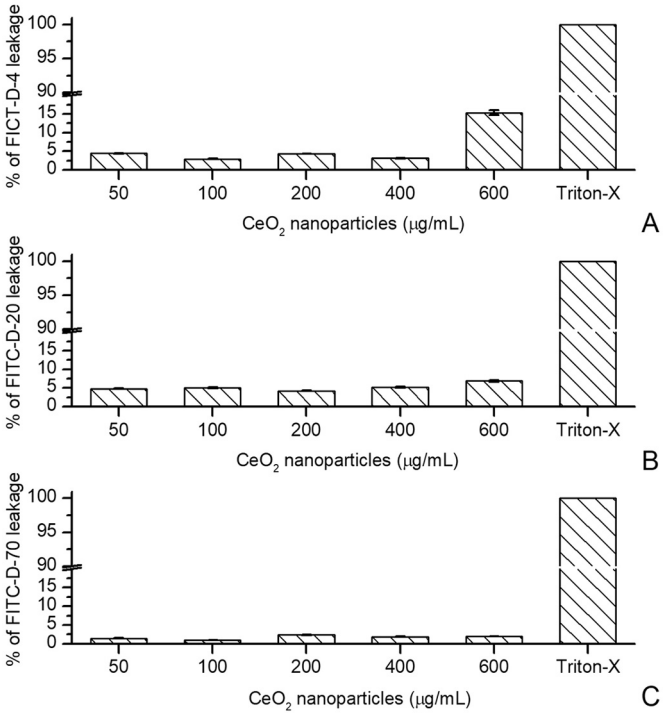

Fig. 3. Percentage of FITC-dextran leakage as function of CeO_2 nanoparticles concentration. D-4 (A), D-20 (B) and D-70 (C) FITC-dextran loaded liposome. Data are presented as mean ± standard deviation (SD).

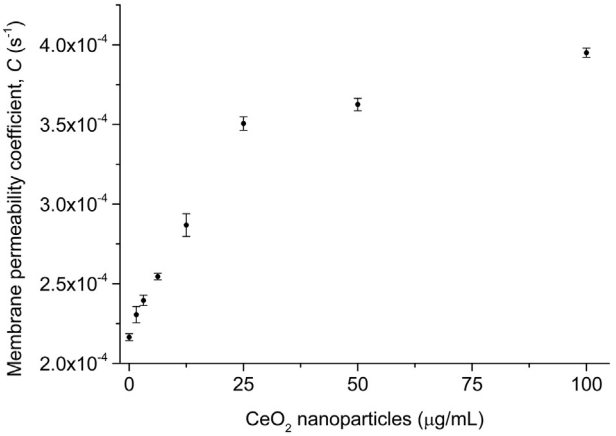

Fig. 4. Plot of the measured coefficient of permeability (*C*) of *Escherichia coli* outer membrane as function of cerium oxide NPs at 50 μM of nitrocefin. Data are presented as mean ± standard deviation (SD).

permeability of Gram-negative bacteria has been assessed by determining the modification of its permeability coefficient (*C*) in presence of several concentrations of cerium oxide NPs. To measure the *C* parameter, the recombinant *E. coli* HB101 producing TEM-1 β-lactamase, has been used as model. β-Lactamases are enzymes able to hydrolyse the β-lactam ring of β-lactam antibiotics. In Gram-negative bacteria, β-lactamases are secreted and confined into the periplasmic space. Nitrocefin is a chromogenic cephalosporin containing a β-lactam nucleus (cephem) that can be used as reporter substrate. Upon hydrolysis, the colour of nitrocefin changes from yellow to red allowing the spectrophotometric identification of the presence of β-lactam hydrolysing enzymes [7].

First, the kinetic parameters for TEM-1 enzyme were determined. The K_m and V_{max} values for nitrocefin were 40.52 ± 3.58 μM and 2.81 ± 0.08 μM/s, respectively.

In these experimental settings, the outer membrane permeability coefficient determined at several cerium oxide NPs concentrations increases as the concentration of cerium oxide NPs becomes higher (Fig. 4). In absence of CeO_2 NPs the value of *C* is equal to $2.16 \times 10^{-3} \pm 2.15 \times 10^{-6}\,s^{-1}$, while it becomes twice at 100 μg/mL of cerium oxide ($C = 3.95 \times 10^{-4} \pm 1.26 \times 10^{-6}\,s^{-1}$).

3.5. In vitro susceptibility and drug interactions

With the purpose of exploiting the possible application in the field of antimicrobial resistance, cerium oxide NPs were tested against multidrug resistant pathogenic *K. pneumoniae*, in combination with therapeutically available β-lactam antibiotics.

As reported in Table 1, *K. pneumoniae* KP1/11 strain showed high levels of resistance against all tested antibiotics. The presence of bla_{KPC-3} and bla_{VIM-2} antibiotic resistance genes, encoding for the serin-β-lactamase KPC-3 and the metallo-β-lactamase VIM-2, respectively, accounts for the reduced susceptibility against imipenem, a carbapenem β-lactam antibiotic, as well as for the high levels of resistance against the combination of amoxicillin, an aminopenicillin β-lactam, and the β-lactamase inhibitor clavulanate. High levels of resistance are also clearly observed for cefotaxime.

Table 1
Minimum inhibitory concentration determined for antibiotics and CeO_2 NPs in *K. pneumoniae* KP1/11. MIC value was determined as the median of three independent experiments.

Antibiotic	MIC (μg/mL)
Cefotaxime	4096
Amoxicillin	1024
Amoxicillin/clavulanate	512/256
Imipenem	128
CeO_2 NPs	> 256

Table 2
In vitro interaction between CeO_2 nanoparticles and beta-lactam antibiotics determined by Δ*E* model in *K. pneumoniae* KP/1/11. **n*, number of drug combinations (among the 77 drug combinations for each strain) with statistically significant synergy or antagonism. Interactions < 100% were considered weak, interactions between 100% and 200% were considered moderate, while interaction > 200% were considered strong. †INT, interpretation; IND indifference; SYN, synergy; ANT, antagonism.

Antibiotic	Δ*E* model		
	ΣSYN (*n*) (%)	ΣANT(*n*)* (%)	INT†
Cefotaxime	679.1 (68)	−5.7 (2)	SYN
Amoxicillin	251.4 (49)	−12.9 (3)	SYN
Amoxicillin/clavulanate	164.6 (21)	−81.8 (14)	SYN
Imipenem	798.2 (44)	−87.7 (14)	SYN

Native CeO_2 NPs are not behaving as antibacterial since no reduction in bacterial growth has been observed at a concentration of 256 μg/mL, the maximum solubility obtained (Table 1).

As shown in Table 2 and in Fig. 5 the interaction between all tested antibiotics and cerium oxide NPs is prevalently synergistic.

As previously mentioned, KP1/11 strain expresses two different carbapenemases. It is interesting to highlight that the highest synergistic activity can be found between imipenem and CeO_2 NPs, with a ΣSYN value of 798,2%. According to Meletiadis et al. [47] interactions < 100% are assumed weak, interactions between 100% and 200% moderate, interaction > 200% strong; thus the combination CeO_2 NPS and imipenem can be considered strong. To this value contributes 44 combinations out of 77 possible combinations (Fig. 5A).

In the same fashion, the combination between cerium oxide NPs and cefotaxime shows a strong synergistic action (Fig. 5B). The combined effect of amoxicillin alone and in combination with the β-lactamase inhibitor clavulanate is significantly lower. In the first case, although a value of ΣSYN of 251,4% (Fig. 5C) can be interpreted as synergistic, is much closer to a moderate action, which is in turn, the synergistic activity that can be found when amoxicillin is combined with clavulanate (Fig. 5D).

4. Discussion

This study aims to investigate the effect of cerium oxide NPs on bacterial outer membrane in Gram-negative bacteria and their potential application in antimicrobial chemotherapy. Although in previous studies have been postulated that CeO_2 NPs interact with the outer membrane of Gram-negative bacterial cells [23,24,28], as also demonstrated by TEM (transmission electronic microscopy) images, the nature and the effects of this interaction were not yet investigated, as well as the antimicrobial activity of certain metal oxide nanoparticles is still under investigation. Nevertheless, several plausible mechanisms of action, or combination of them, have been described [8]. The production of reactive oxygen species (ROS) and damage to cell membrane by electrostatic interaction, seem to be the major modes of action. About the last-mentioned mechanism, the positively-charged metal oxide NPs bind firmly the cell membranes. As previously proposed by Thill [23] the antimicrobial activity of cerium oxide NPs is mainly due to the electrostatic interaction between the negatively-charged bacterial membrane and the positive charge brought by CeO_2 NPs.

In this paper, we have demonstrated that cerium oxide NPs with a diameter of about 10 nm are able to induce a slight permeabilization of biological membranes, without any evident damage. As shown in the calcein-loaded vesicles, the amount of calcein leakage increases in a dose-response manner, as the concentration of CeO_2 NPs increases: the

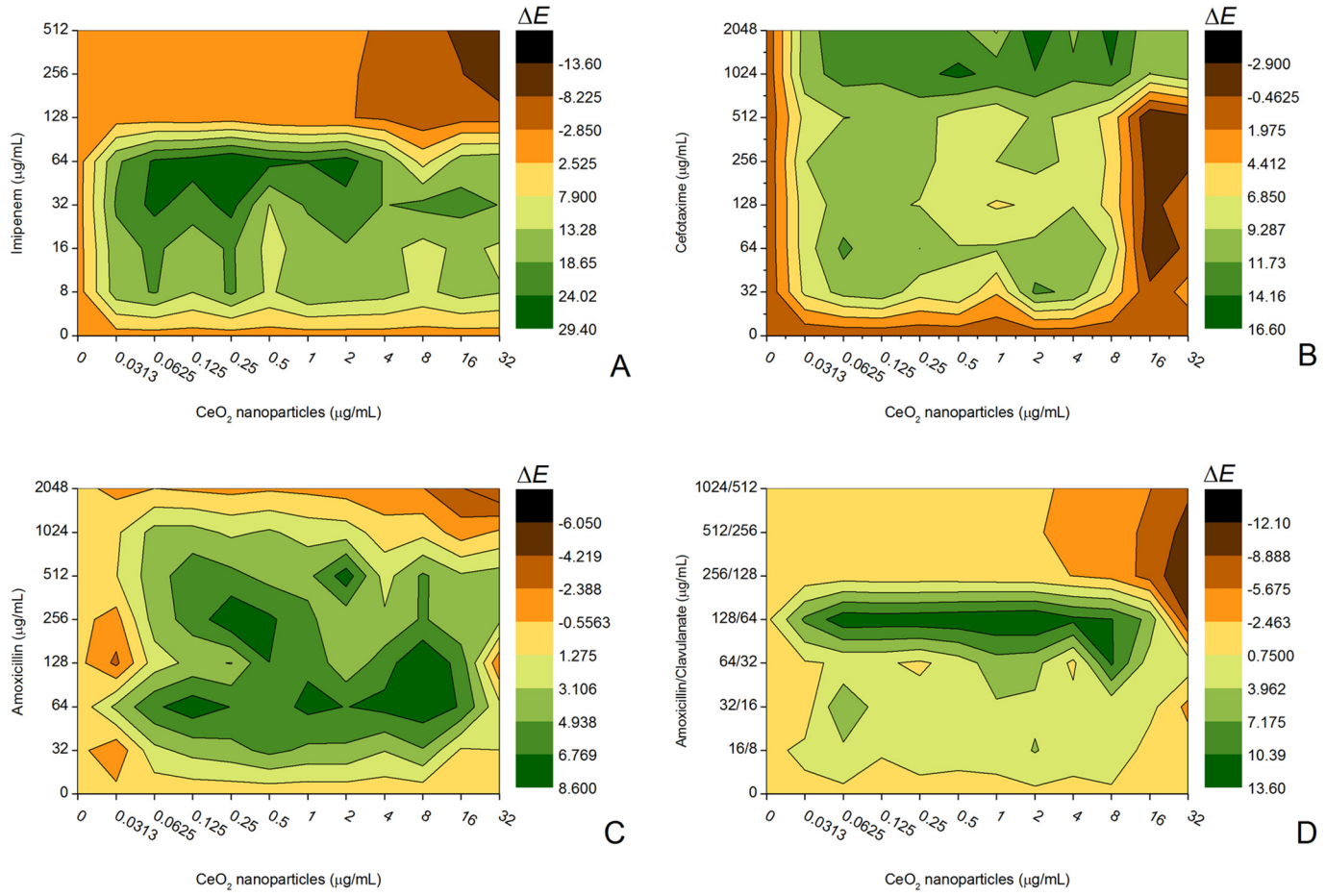

Fig. 5. The three-dimensional plot of the difference between the predicted percentage of growth and the experimental percentage of growth based on the Δ*E* model ($\Delta E = E_{predicted} - E_{measured}$) between CeO_2 NPs and antibiotics against the carbapenem resistant *K. pneumoniae* KP1/11. Combination of cerium oxide NPs with (A), imipenem; (B), cefotaxime; (C), amoxicillin; (D), amoxicillin/clavulanate.

low molecular weight of this compound allows calcein to easily cross the membrane. Despite that, the leakage of calcein is not diagnostic of the entity of perturbation because of the low molecular weight. When lipid vesicles were loaded with higher molecular weight fluorescent probes, precisely FITC conjugate dextrans (D-4, D-20 and D-70), even at highest concentration of cerium oxide NPs, it cannot be possible to observe any significant leakage of the probes.

The absence of dextran leakage is significantly low as the molecular weight increases. This evidence suggests that cerium oxide NPs, at least in multilayer liposomes, are not able to induce meaningful alteration of membrane permeability to induce the leakage of high molecular probes. This is particularly true if compared with calcein leakage. For instance, the low rate release of the 4 kDa FITC-dextran and the almost total absence of 20 kDa and 70 kDa FITC dextran leakage, clearly demonstrate that CeO_2 NPs are not able to disrupt the membrane. Considering that, the leakage of the low molecular weight calcein seems to be related to an increasing permeabilization of the membrane, which allows calcein to pass through.

Data obtained from the loaded liposomes are confirmed by the *in vitro* experiments, where the permeability coefficient of *E. coli* outer membrane toward the low molecular weight nitrocefin (516.5 Da) was determined. The membrane coefficient of permeability increases as the concentration of cerium oxide NPs increases. According to vesicles loaded experiments, the ability of nitrocefin to cross the outer membrane is increased, but at the same time, no beta-lactamase leakage from the periplasmic space is observed. As a matter of fact, TEM-1 beta-lactamase enzyme has a molecular weight approximatively of 25 kDa, as the D-20 dextran.

Macroscopic and nanostructured materials are in the same form such as powder as well as thin films. However, there are intrinsic differences between these two types of materials and these differences determine the material properties. In fact, crystals of macroscopic materials have dimensions between 5 and 100 μm, whereas crystals of nanomaterials have dimensions in the range 5–100 nm. Differences in behaviour are determined by the large difference in grains size. In macroscopic materials the interface between grains represents about 1% of the volume of a polycrystalline object and therefore its influence on the material properties is negligible. On the contrary, nanograins contain a larger number of atoms which are equally distributed between the core and the grain boundary. Therefore, in a nanostructured solid the grain boundary is about 50% of the total volume of the solid itself. Moreover, the structures at the nanometer scale differ from macroscopic materials for a high percentage of atoms on the surface. Therefore, it is very important to consider that the properties of a nanostructured material are strongly influenced by the properties of surface atoms which constitute the interface with the surrounding environment. On the other hand, the electronic states of atoms at the interface and the finite size of the clusters strongly influence the chemical, electronic and optical properties of the nanomaterials.

Our CeO_2 nanoparticles have a core-shell nanostructure in relatively large particles: the core has a composition close to stoichiometric CeO_2 (Ce^{4+}) and the surface is close to Ce_2O_3 (Ce^{3+}). As previously reported [33] the semiquantitative analysis of the Ce 3*d* core-level peak reveals a concentration of Ce^{3+} ions of 24.7%. Therefore, we consider that the composition of our NPs can be schematized as a crystalline CeO_2 (Ce^{4+}) core part and an amorphous Ce_2O_3 (Ce^{3+}) at the surface of the

nanoparticle (Fig. 1). This might be responsible for the high biological activity of nanocrystalline cerium dioxide based on binding of reactive oxygen compounds and radicals deleterious for living systems [11]. Moreover, the positively-charged cerium oxide NPs might displace the divalent cations which stabilise the lipopolysaccharide of the outer membrane, increasing the permeability of the outer membrane to both hydrophobic and hydrophilic substances, as also previously demonstrated for other polycationic molecules [7,48]. The overall result is that the surface area permeable to antibiotic, which is physiologically restricted to porins, is increased allowing the passive diffusion following the concentration gradient. The consequence is the net movement of antibiotic from the area of high concentration, the environment, to the area with lower concentration, the periplasmic space.

As demonstrated by drug interaction experiments on clinical isolate of *K. pneumoniae*, the inactive CeO_2 NPs can exert a synergistic action capable to enhance the activity of β-lactam antibiotics. The simultaneous presence of two different β-lactamase enzymes with carbapenemase activity, as well as high levels of resistance against a broad range of antibacterial, makes the infection caused by this strain difficult to heal with therapeutically available chemotherapeutic agents [49]. In Gram-negative bacteria beta-lactamase enzymes are confined into the periplasmic space and their hydrolytic activity is a function of the permeation of antibiotic across the outer membrane. One of the most important mechanism of resistance in bacteria is for instance the reduction of outer membrane permeability that can be realised by a decreased expression of porins and increased expression of multi-drug efflux pumps [50–53]. Any significant alteration of outer membrane permeability, in the meaning of augmentation, would increase the total uptake of antibiotics into the periplasmic space, which, despite the presence of hydrolytic enzymes, can exert their antimicrobial action.

5. Conclusions

In this paper, we have shown as the inactive cerium oxide NPs, are able to increase the effectiveness of antimicrobials which activity has been compromised by the presence of drug resistance mechanisms. It is plausible to suppose that the synergistic effect is the result of the interaction between cerium oxide NPs and the outer membrane of the bacterial cell. Moreover, the demonstrated low toxicity of CeO_2 NPs, makes them attractive as potential antibiotic adjuvants against MDR pathogenic organisms [11,20,54,55].

The effect of the interaction between cerium oxide NPs and lipid membrane was also investigated to understand how extended the damage is. The use of fluorescent molecular probes with molecular weights ranging from 4 kDa to 70 kDa, allowed to determine that 10 nm cerium oxide NPs, which amorphous (Ce^{3+}) surface represents about 25% of total structure, act as permeabilizers, rather than as “membrane disruptors”, allowing the entrance of the antibiotics, at least in Gram-negative bacteria, according to its gradient of concentration.

The new frontier of antimicrobial chemotherapy is, nowadays, to try to revert antibacterial resistance by combination of drugs, to make old and inactive molecules useful in clinical practice [4]. Of interest is to combine drugs which effectiveness has been compromised by the development and acquisition of multi-drug resistance mechanisms. The idea that the efficacy of a “lost” antibiotic can be retrieved, seems to be today the only rescue strategy capable of fighting infections sustained by MDR pathogenic bacteria.

Conflict of interest

This research did not receive any specific grant from funding agencies in the public, commercial or not-for-profit sectors.

Transparency document

The Transparency document associated with this article can be found, in online version.

References

[1] L.L. Silver, Challenges of antibacterial discovery, Clin. Microbiol. Rev. 24 (2011) 71–109.
[2] G.D. Wright, A.D. Sutherland, New strategies for combating multidrug-resistant bacteria, Trends Mol. Med. 13 (2007) 260–267.
[3] G. Cottarel, J. Wierzbowski, Combination drugs, an emerging option for antibacterial therapy, Trends Biotechnol. 25 (2007) 547–555.
[4] N. Pougat, S. Khatri, A. Singh, M. Dangi, M. Kumar, R. Dabur, A.K. Chhillar, Combination therapy: the propitious rationale for drug development, Comb. Chem. High Throughput Screen. 17 (2014) 53–67.
[5] R.E. Hancock, The *Pseudomonas aeruginosa* outer membrane permeability barrier and how to overcome it, Antibiot. Chemother. (1971) 36 (1985) 95–102.
[6] R.E. Hancock, Peptide antibiotics, Lancet 349 (1997) 418–422.
[7] R.E. Hancock, P.G. Wong, Compounds which increase the permeability of the *Pseudomonas aeruginosa* outer membrane, Antimicrob. Agents Chemother. 26 (1984) 48–52.
[8] A. Raghunath, E. Perumal, Metal oxide nanoparticles as antimicrobial agents: a promise for the future, Int. J. Antimicrob. Agents 49 (2017) 137–152.
[9] O. Mahapatra, M. Bhagat, C. Gopalakrishnan, K.D. Arunachalam, Ultrafine dispersed CuO nanoparticles and their antibacterial activity, J. Exp. Nanosci. 3 (2008) 185–193.
[10] N. Jones, B. Ray, K.T. Ranjit, A.C. Manna, Antibacterial activity of ZnO nanoparticle suspensions on a broad spectrum of microorganisms, FEMS Microbiol. Lett. 279 (2008) 71–76.
[11] S. Das, J.M. Dowding, K.E. Klump, J.F. McGinnis, W. Self, S. Seal, Cerium oxide nanoparticles: applications and prospects in nanomedicine, Nanomedicine 8 (2013) 1483–1508.
[12] V. Shah, S. Shah, H. Shah, F.J. Rispoli, K.T. McDonnell, S. Workeneh, A. Karakoti, A. Kumar, S. Seal, Antibacterial activity of polymer coated cerium oxide nanoparticles, PLoS One 7 (2012) e47827.
[13] A. Cimini, B. Dangelo, S. Das, R. Gentile, E. Benedetti, V. Singh, A.M. Monaco, S. Santucci, S. Seal, Antibody-conjugated PEGylated cerium oxide nanoparticles for specific targeting of Aβ aggregates modulate neuronal survival pathways, Acta Biomater. 8 (2012) 2056–2067.
[14] L.L. Wong, S.M. Hirst, Q.N. Pye, C.M. Reilly, S. Seal, J.F. McGinnis, Catalytic nanoceria are preferentially retained in the rat retina and are not cytotoxic after intravitreal injection, PLoS One 8 (2013) e58431.
[15] L. Alili, M. Sack, C. von Montfort, S. Giri, S. Das, K.S. Carroll, K. Zanger, S. Seal, P. Brenneisen, Downregulation of tumor growth and invasion by redox-active nanoparticles, Antioxid. Redox Signal. 19 (2013) 765–778.
[16] M. Das, S. Patil, N. Bhargava, J.F. Kang, L.M. Riedel, S. Seal, J.J. Hickman, Autocatalytic ceria nanoparticles offer neuroprotection to adult rat spinal cord neurons, Biomaterials 28 (2007) 1918–1925.
[17] B.C. Schanen, S. Das, C.M. Reilly, W.L. Warren, W.T. Self, S. Seal, D.R. Drake, Immunomodulation and T helper TH1/TH2 response polarization by CeO2 and TiO2 nanoparticles, PLoS One 8 (2013) e62816.
[18] G. Pulido-Reyes, I. Rodea-Palomares, S. Das, T.S. Sakthivel, F. Leganes, R. Rosal, S. Seal, F. Fernández-Pinãs, Untangling the biological effects of cerium oxide nanoparticles: the role of surface valence states, Sci. Rep. 5 (2015) 15613.
[19] J.M. Perez, A. Asati, S. Nath, C. Kaittanis, Synthesis of biocompatible dextran-coated nanoceria with pH-dependent antioxidant properties, Small 4 (2008) 552–556.
[20] I. Celardo, J.Z. Pedersen, E. Traversa, L. Ghibelli, Pharmacological potential of cerium oxide nanoparticles, Nanoscale 3 (2011) 1411–1420.
[21] S.S. Lee, H.G. Zhu, E.Q. Contreras, A. Prakash, H.L. Puppala, V.L. Colvin, High temperature decomposition of cerium precursors to form ceria nanocrystal libraries for biological applications, Chem. Mater. 24 (2012) 424–432.
[22] Q. Wang, J.M. Perez, T.J. Webster, Inhibited growth of *Pseudomonas aeruginosa* by dextran- and polyacrylic acid-coated ceria nanoparticles, Int. J. Nanomedicine 8 (2013) 3395–3399.
[23] A. Thill, O. Zeyons, O. Spalla, F. Chauvat, J. Rose, M. Auffan, A.M. Flank, Cytotoxicity of CeO2 nanoparticles for *Escherichia coli* physico-chemical insight of the cytotoxicity mechanism, Environ. Sci. Technol. 40 (2006) 6151–6156.
[24] D.A. Pelletier, A.K. Suresh, G.A. Holton, C.K. McKeown, W. Wang, B. Gu, N.P. Mortensen, D.P. Allison, D.C. Joy, M.R. Allison, S.D. Brown, T.J. Phelps, M.J. Doktycz, Effects of engineered cerium oxide nanoparticles on bacterial growth and viability, Appl. Environ. Microbiol. 76 (2010) 7981–7989.
[25] T. Xia, M. Kovochich, J. Brant, M. Hotze, J. Sempf, T. Oberley, C. Sioutas, J.I. Yeh, M.R. Wiesner, A.E. Nel, Comparison of the abilities of ambient and manufactured nanoparticles to induce cellular toxicity according to an oxidative stress paradigm, Nano Lett. 6 (2006) 1794–1807.
[26] T. Xia, M. Kovochich, M. Liong, L. Mädler, B. Gilbert, H. Shi, J.I. Yeh, J.I. Zink, A.E. Nel, Comparison of the mechanism of toxicity of zinc oxide and cerium oxide nanoparticles based on dissolution and oxidative stress properties, ACS Nano 2 (2008) 2121–2134.
[27] E. Burello, A.P. Worth, A theoretical framework for predicting the oxidative stress potential of oxide nanoparticles, Nanotoxicology 5 (2011) 228–235.
[28] Y. Kuang, X. He, Z. Zhang, Y. Li, H. Zhang, Y. Ma, Z. Wu, Z. Chai, Comparison study on the antibacterial activity of nano- or bulk-cerium oxide, J. Nanosci. Nanotechnol. 11 (2011) 4103–4108.
[29] A. Arumugam, C. Karthikeyan, A.S. Haja Hameed, K. Gopinath, S. Gowri, V. Karthika, Synthesis of cerium oxide nanoparticles using *Gloriosa superba* L. leaf

extract and their structural, optical and antibacterial properties, Mater. Sci. Eng. C Mater. Biol. Appl. 49 (2015) 408–415.
[30] L.P. Babenko, N.M. Zholobak, A.B. Shcherbakov, S.I. Voychuk, L.M. Lazarenko, M.Y. Spivak, Antibacterial activity of cerium colloids against opportunistic microorganisms in vitro, Mikrobiol. Z. 74 (2012) 54–62.
[31] M. Perilli, C. Bottoni, A. Grimaldi, B. Segatore, G. Celenza, M. Mariani, P. Bellio, P. Frascaria, G. Amicosante, Carbapenem-resistant *Klebsiella pneumoniae* harbouring blaKPC-3and blaVIM-2from central Italy, Diagn. Microbiol. Infect. Dis. 75 (2013) 218–221.
[32] H.I. Chen, H.Y. Chang, Synthesis and characterization of nanocrystalline cerium oxide powders by two-stage non-isothermal precipitation, Solid State Commun. 133 (2005) 593–598.
[33] M. Passacantando, S. Santucci, Surface electronic and structural properties of CeO2 nanoparticles: a study by core-level photoemission and peak diffraction, J. Nanopart. Res. 15 (2013).
[34] M.L. Mangoni, A.C. Rinaldi, A. Di Giulio, G. Mignogna, A. Bozzi, D. Barra, M. Simmaco, Structure-function relationships of temporins, small antimicrobial peptides from amphibian skin, Eur. J. Biochem. 267 (2000) 1447–1454.
[35] F. Szoka, D. Papahadjopoulos, Procedure for preparation of liposomes with large internal aqueous space and high capture by reverse-phase evaporation, Proc. Natl. Acad. Sci. U. S. A. 75 (1978) 4194–4198.
[36] J.C. Stewart, Colorimetric determination of phospholipids with ammonium ferrothiocyanate, Anal. Biochem. 104 (1980) 10–14.
[37] K. Matsuzaki, K. Sugishita, K. Miyajima, Interactions of an antimicrobial peptide, magainin 2, with lipopolysaccharide-containing liposomes as a model for outer membranes of gram-negative bacteria, FEBS Lett. 449 (1999) 221–224.
[38] A.C. Rinaldi, A. Di Giulio, M. Liberi, G. Gualtieri, A. Oratore, A. Bozzi, M.E. Schininà, M. Simmaco, Effects of temporins on molecular dynamics and membrane permeabilization in lipid vesicles, J. Pept. Res. 58 (2001) 213–220.
[39] W. Zimmermann, A. Rosselet, Function of the outer membrane of *Escherichia coli* as a permeability barrier to beta-lactam antibiotics, Antimicrob. Agents Chemother. 12 (1977) 368–372.
[40] H.E. Villar, F. Danel, D.M. Livermore, Permeability to carbapenems of *Proteus mirabilis* mutants selected for resistance to imipenem or other beta-lactams, J. Antimicrob. Chemother. 40 (1997) 365–370.
[41] CLSI, Performance standards for antimicrobial susceptibility testing, Twenty-first Informational Supplement M100-S21, 2010.
[42] G. Celenza, B. Segatore, D. Setacci, P. Bellio, F. Brisdelli, M. Piovano, J.A. Garbarino, M. Nicoletti, M. Perilli, G. Amicosante, In vitro antimicrobial activity of pannarin alone and in combination with antibiotics against methicillin-resistant *Staphylococcus aureus* clinical isolates, Phytomedicine 19 (2012) 596–602.
[43] B. Segatore, P. Bellio, D. Setacci, F. Brisdelli, M. Piovano, J.A. Garbarino, M. Nicoletti, G. Amicosante, M. Perilli, G. Celenza, In vitro interaction of usnic acid in combination with antimicrobial agents against methicillin-resistant Staphylococcus aureus clinical isolates determined by FICI and Δe model methods, Phytomedicine 19 (2012).
[44] W.R. Greco, G. Bravo, J.C. Parsons, The search for synergy: a critical review from a response surface perspective, Pharmacol. Rev. 47 (1995) 331–385.
[45] M.N. Prichard, L.E. Prichard, W.A. Baguley, M.R. Nassiri, C. Shipman, Three-dimensional analysis of the synergistic cytotoxicity of ganciclovir and zidovudine, Antimicrob. Agents Chemother. 35 (1991) 1060–1065.
[46] M.N. Prichard, C. Shipman, A three-dimensional model to analyze drug-drug interactions, Antivir. Res. 14 (1990) 181–205.
[47] J. Meletiadis, P.E. Verweij, D.T. TeDorsthorst, J.F. Meis, J.W. Mouton, Assessing in vitro combinations of antifungal drugs against yeasts and filamentous fungi: comparison of different drug interaction models, Med. Mycol. 43 (2005) 133–152.
[48] M.G. Scott, H. Yan, R.E. Hancock, Biological properties of structurally related alpha-helical cationic antimicrobial peptides, Infect. Immun. 67 (1999) 2005–2009.
[49] L.S. Tzouvelekis, A. Markogiannakis, M. Psichogiou, P.T. Tassios, G.L. Daikos, Carbapenemases in *Klebsiella pneumoniae* and other Enterobacteriaceae: an evolving crisis of global dimensions, Clin. Microbiol. Rev. 25 (2012) 682–707.
[50] X.Z. Li, H. Nikaido, Efflux-mediated drug resistance in bacteria: an update, Drugs 69 (2009) 1555–1623.
[51] H. Nikaido, Molecular basis of bacterial outer membrane permeability revisited, Microbiol. Mol. Biol. Rev. 67 (2003) 593–656.
[52] K. Poole, Efflux-mediated antimicrobial resistance, J. Antimicrob. Chemother. 56 (2005) 20–51.
[53] L.J. Piddock, Clinically relevant chromosomally encoded multidrug resistance efflux pumps in bacteria, Clin. Microbiol. Rev. 19 (2006) 382–402.
[54] B. Park, K. Donaldson, R. Duffin, L. Tran, F. Kelly, I. Mudway, J.P. Morin, R. Guest, P. Jenkinson, Z. Samaras, M. Giannouli, H. Kouridis, P. Martin, Hazard and risk assessment of a nanoparticulate cerium oxide-based diesel fuel additive - a case study, Inhal. Toxicol. 20 (2008) 547–566.
[55] N. O'Brien, E. Cummins, Ranking initial environmental and human health risk resulting from environmentally relevant nanomaterials, J. Environ. Sci. Health A Tox. Hazard. Subst. Environ. Eng. 45 (2010) 992–1007.